Trends in semiconductor laser design: Balance between leakage, gain and loss in InGaAsP/InP MQW structures.

G. Belenky, L. Shterengas
State University of New York at Stony Brook, Stony Brook, NY 11794 USA
garik@ece.sunysb.edu

C.W. Trussell
Night Vision & Electronic Sensors Directorate, 10215 Burbeck Road, Ft Belvoir, VA 22060-5806 USA

C.L. Reynolds, Jr.
Agere Systems, Breinigsville, PA 18031 USA

M.S. Hybertsen
Agere Systems, Murray Hill, NJ 07974 USA

R. Menna
Princeton Lightwave Inc., Cranbury, NJ 08512 USA

Abstract

The trade-off between the effect of leakage suppression and the increase of related optical loss due to placement of the p-doping in 1.3-1.55μm InGaAsP MQW edge-emitting lasers is detailed. The effect of the Zn doping profile on laser characteristics is illustrated by experimental results obtained for telecom lasers and high power lasers. The design approach combining broadened waveguides with p-doping profile optimization is discussed. 16W of pulsed optical power is obtained from 100μm aperture 1.5μm InGaAsP MQW high power lasers with broadened waveguide and doped p-cladding/SCH interface.

Introduction

InGaAsP/InP is one of the basic material systems of modern optoelectronics. Well-developed and mature MOCVD technology allows for high yield fabrication of lasers in the wavelength range from 0.97 and up to 2μm for telecom and other needs. The main peculiarity of devices based on InGaAsP is a relatively small conduction band offset; about 60% of the net band offset is valence band offset. The high mobility of electrons together with a rather small confinement barrier makes carrier leakage through thermionic emission a serious concern.

Modern semiconductor laser design approaches extensively use doping profile and waveguide geometry tuning. In this paper we will consider in detail both of these design tools. Experimental demonstration of their successful application to 1.3μm and 1.5μm InGaAsP/InP MQW lasers will be shown.

Doping of the p-cladding/SCH interface is a powerful tool for heterobarrier carrier leakage suppression leading to high injection efficiency [1]. The introduction of p-doping into the waveguide or even the active region increases device temperature stability and improves high frequency performance [2,3]. The price paid for these advantages is an increased optical loss due to free carrier absorption. Alternatively, waveguide broadening minimizes optical loss due to the decreased overlap of the optical mode with the highly doped cladding regions [4]. The trade-off between increased loss and the reduction of carrier leakage from the active region governs laser design. When high modulation bandwidth is an issue device design is further complicated by carrier transport considerations [1].

Different semiconductor laser applications place various requirements on the device parameters. Telecom transmitters for digital and analog links need low threshold, high efficiency, low noise, high modulation bandwidth and highly linear light-current (LI) characteristics. It is almost impossible to optimize laser structure for all these purposes simultaneously. However, maximization of the external efficiency and minimization of the threshold current can be achieved for relatively low-doped waveguide but high doped p-clad/SCH interface [1]. Temperature stability preferred for uncooled device operation is reached with higher doping of the waveguide layer [2]. Active region doping, in turn, increases the differential gain thus improving the device high frequency characteristics [3].

For high power lasers, small threshold current, large efficiency and low series resistance are of special importance. Use of the broadened waveguide (BW) approach led to record low values of optical loss boosting device external efficiency and enabled fabrication of the high power devices [4]. The combination of the BW approach with optimization of the doping profile [5] is demonstrated for a 1.5μm high power InGaAsP/InP multiple quantum well (MQW) lasers. A sharp increase of the Zn concentration near the p-clad/SCH interface relaxes the light-current characteristics (LI) rollover keeping the efficiency at a high level.

The paper is subdivided into three parts. Part I explains the role of p-doping profile in InP-based laser structures performance. In Part II experimental data for 1.3μm InGaAsP/InP MQW lasers with optimized p-doping profiles are presented. Part III demonstrates design of 1.5μm InGaAsP/InP MQW lasers in which BW and optimized Zn doping profile approaches are combined.

I. Role of p-doping profile in InP-based laser performance.

Experimental and modeling results obtained by different groups show that changes of acceptor concentration within different regions of the laser structure significantly affect device characteristics. We will consider here the effects of the doping of different regions separately.

1. p-doping of the SCH/p-cladding interface.

Acceptor centers in the vicinity of the SCH/p-cladding interface in InP-based semiconductor laser lead to reduced heterobarrier leakage of the electrons from the waveguide region into the p-cladding. The energy barrier for thermionic emission controls amount of the heterobarrier carrier leakage. Due to the relatively small conduction band offset at the InGaAsP/InP heterobarrier interface and the small electron effective mass, electron leakage current due to thermal emission into the p-cladding can be significant. Hole heterobarrier leakage is not of any concern in this material system due to the large hole effective mass in combination with the higher energy barrier. The effective barrier for thermionic emission of electrons combines the band discontinuity (ΔE_C) and the local band bending resulting from modulation doping effect (fig. 1).

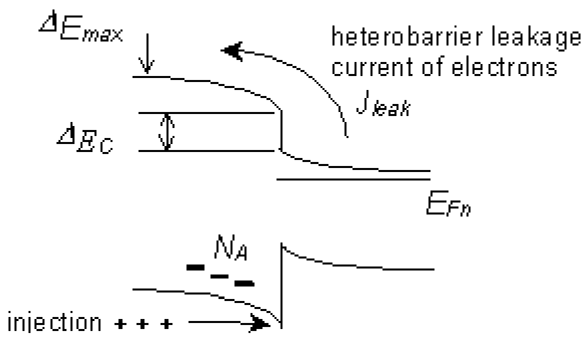

Figure 1. Schematic band diagram of the laser structure in the vicinity of p-cladding/SCH interface: barrier for thermionic emission of electrons.

The leakage current (J_{leak}) depends exponentially on this energy barrier:

$$J_{leak} \propto \exp\left(-\frac{E_c^{\max} - E_{Fn}}{kT}\right), \qquad (1)$$

where E_{Fn} is the electron quasi-Fermi level in the waveguide (SCH) near the interface. The local maximum in the conduction band profile (E_c^{max}) includes band bending related to the local doping concentration (N_A) and the influence of injected carriers due to external voltage drop. Higher doping near the interface reduces this additional voltage drop and, consequently, the heterobarrier leakage. Heterobarrier leakage suppression leads to laser slope efficiency enhancement since the injection efficiency increases.

2. p-doping of the waveguide region.

High Zn concentration in the waveguide (SCH) region suppresses the effect of the electrostatic band bending [6]. The electrostatic band profile deformation was argued to increase device temperature sensitivity. The origin of this effect is separation of the charge in the waveguide. At high injection, electrons can spill over into the SCH region from QWs while holes remain localized within the QW. This separation of charges creates an electrostatic band profile deformation increasing the effective barrier for the conduction band, and decreasing the effective barrier for the valence band. At elevated temperatures, the hole density within the SCH can increase leading to an increase in loss and recombination in the SCH. As a result, this causes a rise of the threshold current and a decrease of the slope efficiency. Incorporation of the acceptors into the waveguide region affects the charge distribution, thus suppressing the accumulation of excess holes in SCH [2].

3. p-doping of the active region.

It was shown theoretically and experimentally that p-doping of the active region in strained MQW InGaAsP/InP lasers can substantially increase the differential gain leading to greater maximum modulation frequency [3,7,8]. Differential gain or, in other words, gain change per each additional injected electron-hole pair is controlled by the carrier energy distribution and the relative position of the quasi-Fermi level with respect to states coupled into the laser mode. In most of the, the lasing transition couples states from approximately the bottom of the conduction band to the top of the valence band. The closer are the quasi-Fermi levels to the band edges in the QW, the higher is the differential gain because population inversion change per each additional electron-hole pair increases. At the transparency current the energy equal to the material energy gap separates the quasi-Fermi levels. Because the effective mass is about one order of magnitude lower for electrons than for holes the electron quasi-Fermi level at transparency is in the conduction band while the hole quasi-Fermi level is in the forbidden gap. With increase of Zn concentration in active region, the quasi-Fermi levels for electrons and holes shift closer to the energy band edges. As a result, differential gain increases. Moreover, tuning of the MQW active region doping profile was argued to reduce carrier transport related impediments [1,9].

Introduction of p-doping into any part of the laser structure overlapped with the optical field leads to increased optical loss through free carrier and intervalence band absorption. This causes the threshold to increase and the slope efficiency to decrease, especially serious concerns in high power lasers.

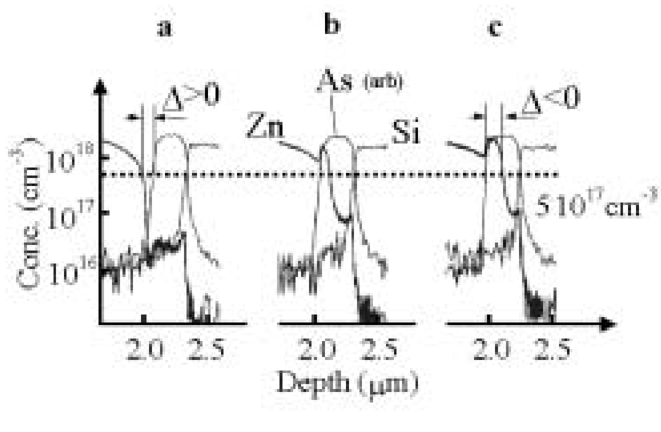

Figure 2. SIMS data for 1.3μm InGaAsP MQW lasers with three different Zn doping profiles: low doped (a), moderately doped (b) and doped (c).

II. Optimization of p-doping profile in 1.3μm InGaAsP/InP MQW lasers.

In [1-3] the study of the effect of p-doping on 1.3μm InGaAsP/InP MQW lasers performance was carried out experimentally. It was shown that there exists an optimum p-i junction placement simultaneously maximizing external efficiency and minimizing threshold current. To define the placement of Zn doping within the laser structure, a setback (Δ) parameter was introduced as the distance between the Zn-doping profile edge at concentration of $5x10^{17}cm^{-3}$, and the p-cladding/SCH. Fig. 2 shows secondary ion mass spectrometry (SIMS) data for devices with three different doping profiles [1]. The dependence of the heterobarrier leakage current on Δ is shown in fig. 3a. In agreement with the analysis given in part I, heterobarrier leakage current vanishes as p-doping intrudes deeper into the waveguide region. At the same time, external efficiency tends to decrease since loss increases with doping due to free carrier absorption. Simulation predicts and experiment confirms that Δ = 50nm is optimum for minimum threshold and maximum external efficiency (fig. 3b).

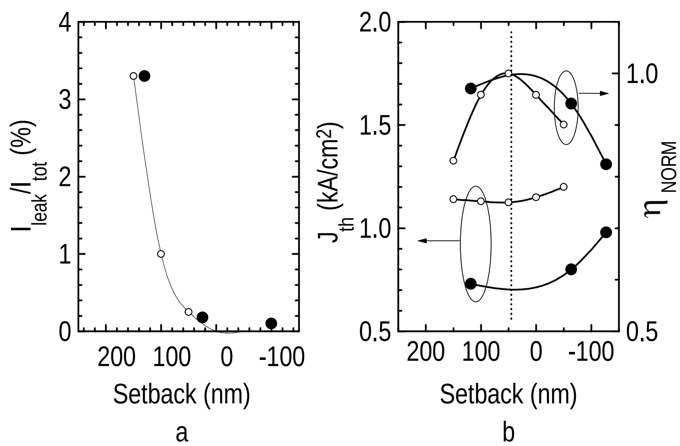

Figure 3. Dependence of the reduced leakage current (a); threshold current density and normalized external efficiency on doping profile. Open dots – simulation, solid dots – experiment.

To minimize the device temperature sensitivity, the value of Δ must be different. As it was pointed out in part I, the effect of electrostatic bend profile deformation can be suppressed by using a doped waveguide. Laser temperature stability can be characterized by the power penalty parameter. It is defined as a change in the output power level caused by ambient temperature change while current through the device is kept constant:

$$\frac{1}{P}\frac{dP}{dT} = \frac{1}{\eta}\frac{d\eta}{dT} - \frac{1}{T_0(m-1)}, \quad m = \frac{I}{I_{th}}, \qquad (2)$$

where P is the output power, and η is the - external efficiency. The second term prevails in the current dependence (fig. 4a). The value of the power penalty decreases with current (fig. 4). Fig. 4b shows that the power penalty is minimized at a negative setback value of about – 50nm or, in other words, when the SCH layer is doped [10]. The price for increased temperature stability is decreased efficiency and increased threshold (see fig. 3b for Δ = - 50nm).

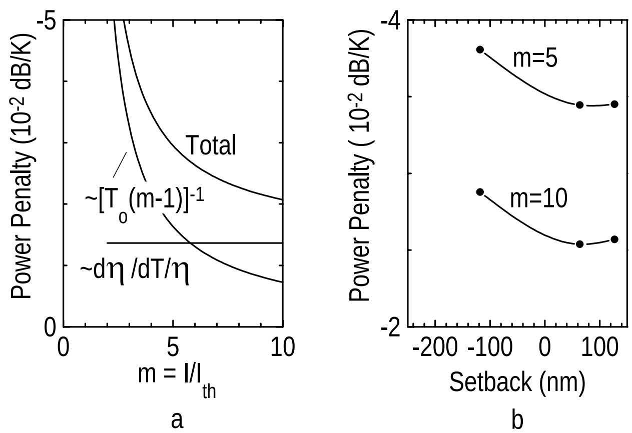

Figure 4. Dependence of the power penalty on pumping (a); power penalty as a function of doping profile (b) for m=5 and m=10.

Finally we will consider the effect of MQW region p-doping on the device differential gain. Fig. 5 shows the temperature dependence of the differential gain for 1.3µm InGaAsP/InP Fabri-Perot (FP, - fig. 5a) and distributed feedback (DFB, - fig. 5b) capped mesa buried heterostructure (CMBH) lasers.

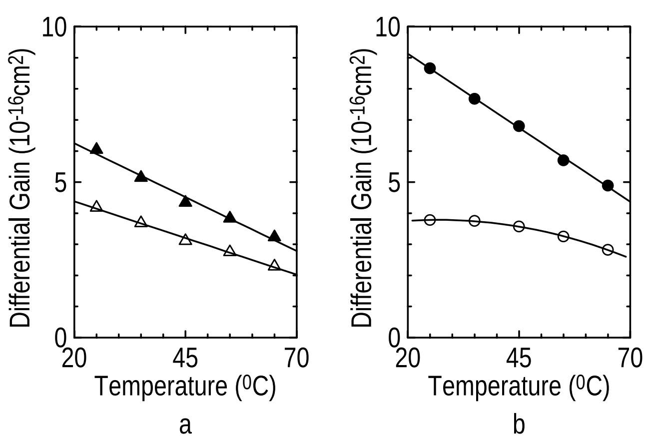

Figure 5. Temperature dependence of the differential gain for moderately doped (open symbols) and doped (solid symbols) FP (a) and DFB (b) lasers.

Results for the devices with two different doping profiles are shown: moderately doped (similar to fig. 2b) and doped (similar to fig. 2c). The shift of the quasi-Fermi levels closer to the band edges with increased p-doping explains the higher differential gain values in the doped compared to the moderately doped structures. However, the temperature sensitivity of the differential gain is enhanced with doping because closeness of the quasi-Fermi level to the electronic states coupled to the laser mode also leads to larger changes of the population inversion with temperature.

The temperature dependence of the differential gain for DFB devices is further influenced by detuning – (defined as the difference between the wavelength of the gain maximum and the lasing wavelength). For a particular operating carrier density in the active layer, the differential gain is a strong function of wavelength, being smaller on the long wavelength side of the gain peak and larger on the short wavelength side [11]. This explains the larger difference in measured differential gain between the moderately (slightly positively detuned) and the heavily doped (negatively detuned) DFB lasers in comparison to the FP lasers. When the lasing wavelength is detuned from the gain peak, then the operating carrier density must be larger which leads to a lower differential gain overall. For the devices studied, the operating carrier density changes with temperature both due to the intrinsic dependence of gain on temperature and due to the change in the spectral position of the lasing mode relative to the gain peak. For the devices with negative detuning (the doped lasers) the rise of temperature leads to additional increase of the operating carrier density due to an increase of the detuning value. In moderately doped devices the increase of temperature decreases positive detuning, thus suppressing the temperature dependence of the differential gain up to about 40^0C. After this temperature the effect of the operating carrier density becomes apparent again.

III. Effect of doping profile on performance of high power 1.5μm InGaAsP MQW BW lasers.

The BW design decreases the internal optical loss leading to improved slope efficiency at threshold. The loss decrease is achieved through reduced overlap of the optical field with highly doped cladding layers. Reduction of the mode confinement with MQW region with waveguide broadening is counterbalanced by the significant optical loss decrease [4]. The devices with BW exhibit improved external efficiency at low injection current. However, at high injection, thermal rollover limits the output power level. It was shown experimentally [12] that the heterobarrier leakage current contributes to the LI rollover of 1.5μm InGaAsP/InP narrow waveguide lasers. In this part of the paper we present new data showing that the doping of p-cladding/SCH interface of 1.5μm InGaAsP/InP BW high power lasers suppresses LI rollover leading to higher output power.

Broadened waveguide lasers with three different doping profiles were fabricated. The design of the lasers was similar to the one used in Ref. 4. The structure is MOCVD grown on n-InP substrate. Active region contains 3 InGaAsP QWs (4.5nm) with 1% of compressive strain separated by 16nm InGaAsP barriers. An InGaAsP double step graded index separate confinement heterostructure (SCH) provides optical confinement. The total width of the broadened waveguide (W) region is 710nm. All layers but the QWs are lattice matched to InP. The waveguide is sandwiched between 1.5μm InP cladding layers. Lasers with three different Zn doping levels of p-cladding/SCH interface were tested. The corresponding SIMS data for the studied broad area 1.5-μm InGaAsP/InP MQW BW lasers are shown in Fig. 6.

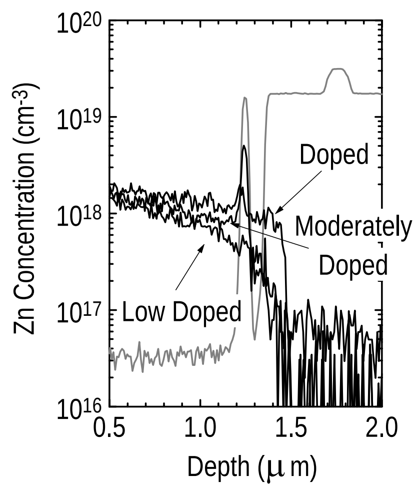

Figure 6. SIMS data for 1.5μm InGaAsP MQW broadened waveguide lasers with three different Zn doping profiles.

The device front and back mirrors were coated with low (3-5%) and high reflectivity (95%), respectively. In order to minimize thermal effects, low duty cycles (less than 0.1%) and short current pulses (100-200ns) were used. The two main effects of doping on LI are shown in Fig. 7a. First, the slope efficiency at threshold steadily decreases with doping suggesting higher optical loss for doped devices. Second, the effect of power saturation at high current densities decreases with increased doping levels, which confirms the suppression of heterobarrier leakage.

We measured directly the current dependence of the modal gain spectra of the lasers studied (Fig. 8). A spatial filtering [13,14] selected on-axis optical modes of the multimode broad area lasers. Amplified spontaneous emission (ASE) spectra were monitored using a Fourier transform spectrometer (MAGNA860). Modal gain spectra were obtained from the ASE spectra by the Hakki-Paoli method [15]. In the energy region where modal gain saturates (the range of low photon energies in Fig. 8) the material gain is equal to zero and modal gain is equal to the total optical loss. Subtracting the calculated mirror loss (about $18cm^{-1}$ and $36cm^{-1}$ for 1mm and 500μm cavity length devices correspondingly) from the experimentally determined total optical loss, we obtain the internal optical loss value. Lasers with the lowest Zn concentration in the vicinity of the p-cladding/SCH interface have about $4cm^{-1}$ internal optical losses (fig. 8a). As Zn propagates deeper into the waveguide, the internal loss goes up to $12cm^{-1}$ for the doped devices (fig. 8c).

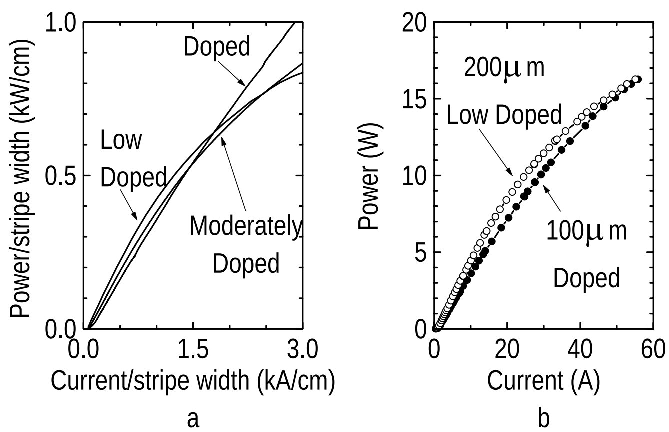

Figure 7. Dependence of the output optical power per stripe width on current per stripe width for devices with three different doping profiles (a); Light-current characteristics for low doped 200μm stripe width and doped 100μm stripe width lasers (b).

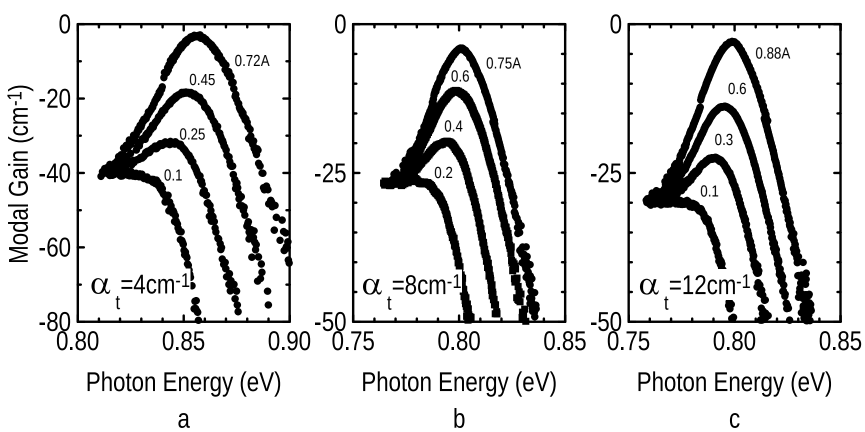

Figure 8. Current dependence of the modal gain spectra for low doped (a), moderately doped (b) and doped (c) lasers.

At high injection levels when the barrier for electron thermionic emission from SCH into p-cladding is suppressed by the external voltage, heterobarrier leakage increases and the LI saturates. Optimization of the device p-doping profile allowed us to obtain the same output optical power from 100μm BW doped lasers as from 200μm BW low-doped ones (Fig. 7b). Far field emission patterns were almost independent of stripe width and doping profile with about 20^0x50^0 divergence for high output power levels. Due to better linearity of LI characteristics, the BW doped lasers yielded twice the output optical power density and brightness as BW low-doped devices at 60A.

Authors would like to acknowledge Dmitry Donetsky for valuable discussion and ARO grant DAAD190010423 for support.

References

1. G.L. Belenky, C.L. Reynolds, Jr., D.V. Donetsky, G.E. Shtengel, M. Hybertsen, M.A. Alam, G.A. Baraff, R.K. Smith, R.F. Kazarinov, J. Winn, L.E. Smith "Role of p-doping profile and regrowth on the static characteristics of 1.3 mm MQW InGaAsP/InP lasers. Experiment and modeling" *IEEE J. Quantum. Electron.* **35** (1999), pp. 1515-1520.
2. G.L. Belenky, D.V. Donetsky, C.L. Reynolds, Jr., R.F. Kazarinov, G.E. Shtengel, S. Luryi, J. Lopata, "Temperature performance of 1.3-μm InGaAsP-InP lasers with different profile of p-doping", *IEEE Photon. Tech. Lett.* **9** (1997), pp. 1558-1560
3. G. Belenky, C.L. Reynolds, Jr., L. Shterengas, M.S. Hybertsen, D.V. Donetsky, G.E. Shtengel, and S. Luryi "Effect of p-doping on temperature dependence of differential gain in FP and DFB 1.3μm InGaAsP/InP multiple quantum well lasers" *IEEE Photon. Tech. Lett.* **12**(2000), pp. 969-971.
4. D.Z. Garbuzov, R.J. Menna, R.U. Martinelli, J.H. Abeles, J.C. Connolly "High power continuous and quasi-continuous wave InGaAsP/InP broad-waveguide separate confinement-heterostructure lasers" *IEE Electron. Lett.* **33** (1997), pp. 1635-1636.
5. I.K Han, S.H. Cho, P.J.S. Heim, D.H. Woo, S.H. Kim, J.H. Song, F.G. Johnson, M. Dagenais, "Dependence of the light-current characteristics of 1.55-μm broad-area lasers on different p-doping profiles", *IEEE Photon. Tech. Lett.* **12** (2000), pp. 251-253.
6. S. Seki, K. Yokoyama, "Electrostatic deformation in band profiles of InP-based strained-layer quantum well lasers", *J. Appl. Phys.* **77** (1995), pp. 5180-5184.
7. T. Yamanaka, Y. Yoshikuni, K. Yokoyama, W. Lui, S. Seki, "Theoretical study on enhanced differential gain and extremely reduced linewidth enhancement factor in quantum-well lasers", *IEEE J. Quantum. Electron.* **29**, (1993), pp. 1609-1616.
8. I.F. Lealman, M.J. Harlow, S.D. Perrin, "Effect of Zn doping on modulation bandwidth of 1.55μm InGaAs/InGaAsP multiplequantum well lasers", *Electron. Lett.* **29** (1993), pp. 1197-1198.
9. M.A. Alam, M.S. Hybertsen, R.K. Smith, G.A. Baraff, "Simulation of Semiconductor Quantum Well Lasers", IEEE Transaction on Electron Devices 47 (2000), pp. 1917-1925.

---

10. D. Donetsky, “Temperature performance of InP and GaSb-based laser diodes”, *PhD thesis, SUNY at Stony Brook* (2000).
11. P.A. Morton, D.A. Ackerman, G.E. Shtengel, R.F. Kazarinov, M.S. Hybertsen, T. Tanbun-Ek, R.A. Logan, and A.M. Sergent, “Gain characteristics of 1.55-μm high-speed multiple-quantum-well lasers,” *IEEE Photon. Tech. Lett.* **7** (1995), pp. 833-835.
12. L. Shterengas, R. Menna, W. Trussell, D. Donetsky, G. Belenky, J. Connolly, D. Garbuzov “Effect of heterobarrier leakage on the performance of high power 1.5-μm InGaAsP MQW lasers”. *J. Appl. Phys*. **88** (2000), pp. 2211-2214.
13. Bossert D.J., Gallant D., “Improved method for gain/index measurements of semiconductor lasers.” *Electron Lett*,, **32** (1996), pp. 338-339.
14. D.V. Donetsky, G.L. Belenky, D.Z. Garbuzov, H. Lee, R.U. Martinelli, G. Taylor, S. Luryi, J.C. Connolly, "Direct measurements of heterobarrier leakage current and modal gain in 2.3μm double QW p-substrate InGaAsSb/AlGaAsSb broad area lasers", *IEE Electron. Lett.,* **35** (1999), pp. 298-299.
15. B.W. Hakki and T.L. Paoli, “CW degradation at 300K of GaAs double-heterostructure junction lasers. II. Electronic gain.”, *J. Appl. Phys.* **44** (1973) 4113-4119.